Science of the Total Environment 862 (2023) 160771

Contents lists available at ScienceDirect

Science of the Total Environment

journal homepage: www.elsevier.com/locate/scitotenv

Seasonal variation of driving factors of ambient $PM_{2.5}$ oxidative potential in Shenzhen, China

Chunbo Xing [a,b], Yixiang Wang [b], Xin Yang [b,c,*], Yaling Zeng [b], Jinghao Zhai [b], Baohua Cai [b], Antai Zhang [b], Tzung-May Fu [b], Lei Zhu [b], Ying Li [d], Xinming Wang [e], Yanli Zhang [e]

[a] School of Environment, Harbin Institute of Technology, Harbin 150001, China
[b] Shenzhen Key Laboratory of Precision Measurement and Early Warning Technology for Urban Environmental Health Risks, School of Environmental Science and Engineering, Southern University of Science and Technology, Shenzhen 518055, China
[c] Guangdong Provincial Observation and Research Station for Coastal Atmosphere and Climate of the Greater Bay Area, Shenzhen, Guangdong 518055, China
[d] Department of Ocean Sciences and Engineering, Southern University of Science and Technology, Shenzhen 518055, China
[e] State Key Laboratory of Organic Geochemistry, Guangdong Key Laboratory of Environmental Protection and Resources Utilization, Guangzhou Institute of Geochemistry, Chinese Academy of Sciences, Guangzhou 510640, China

HIGHLIGHTS

- Oxidative potential of 132 $PM_{2.5}$ samples covering winter and summer were measured.
- Seasonal weather condition change exerts huge impacts on $PM_{2.5}$ and its OP.
- Long-range transport biomass burning and ship emissions dominate the $PM_{2.5}$ OP.
- Dithiothreitol depletion and •OH generation can complementarily assess the $PM_{2.5}$ OP.

GRAPHICAL ABSTRACT

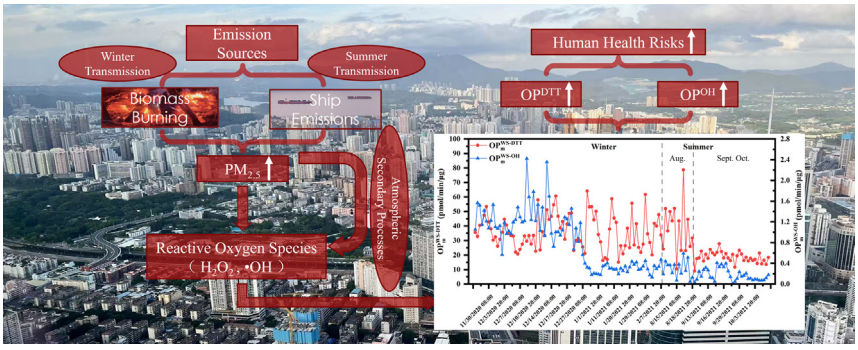

ARTICLE INFO

Editor: Jianmin Chen

Keywords:
Dithiothreitol
Hydroxyl radical
$PM_{2.5}$
Oxidative potential
Emission source
Seasonal variation

ABSTRACT

Reactive oxygen species (ROS) play a central role in health effects of ambient fine particulate matter ($PM_{2.5}$). In this work, we screened for efficient and complementary oxidative potential (OP) measurements by comparing the response values of multiple chemical probes (OP^{DTT}, OP^{OH}, OP^{GSH}) to ambient $PM_{2.5}$ in Shenzhen, China. Combined with meteorological condition and $PM_{2.5}$ chemical composition analysis, we explored the effects of different chemical components and emission sources on the ambient $PM_{2.5}$ OP and analyzed their seasonal variations. The results show that OP_m^{DTT}(mass-normalized) and $OP_m^{GSH-SLF}$ were highly correlated ($r = 0.77$). OP^{DTT} was mainly influenced by organic carbon, while OP^{OH} was highly dominated by heavy metals. The combination of OP^{DTT} and OP^{OH} provides an efficient and comprehensive measurement of OP. Temporally, the OPs were substantially higher in winter than in summer (1.4 and 4 times higher for OP_m^{DTT} and OP_m^{OH}, respectively). The long-distance transported biomass burning sources from the north dominated the OP^{DTT} in winter, while the ship emissions mainly influenced the summer OP. The OP_m^{DTT} increased sharply with the decrease of $PM_{2.5}$ mass concentration, especially when the $PM_{2.5}$ concentration was lower than 30 μg/m^3. The huge differences in wind fields between the winter and summer cause considerable variations in $PM_{2.5}$ concentrations, components, and OP. Our work emphasizes the necessity of long-term, multi-method, multi-component assessment of the OP of $PM_{2.5}$.

* Corresponding author at: Southern University of Science and Technology, School of Environmental Science and Engineering, No. 1088 Xueyuan Avenue, Nanshan District, Shenzhen, Guangdong Province, China.
E-mail address: yangx@sustech.edu.cn (X. Yang).

http://dx.doi.org/10.1016/j.scitotenv.2022.160771
Received 8 November 2022; Received in revised form 1 December 2022; Accepted 4 December 2022
Available online 10 December 2022

1. Introduction

Epidemiological and toxicological studies have shown that ambient $PM_{2.5}$ (particles with aerodynamic diameters <2.5 μm) can cause adverse health problems such as respiratory and cardiovascular diseases (Bates et al., 2015; Abrams et al., 2017; Maikawa et al., 2016; Pope et al., 2015; He et al., 2021; Liu et al., 2018; Crobeddu et al., 2020). $PM_{2.5}$ causes 7 million premature deaths globally each year (He and Zhang, 2022). However, the mechanisms of the toxic effects of particulate matter on human health are not fully understood. Growing evidence shows that exposure to particulate matter induces oxidative stress in the body (Li et al., 2003; Strak et al., 2012; Saffari et al., 2014), providing a potential mechanism of toxicity for PM, and oxidative stress is the most widely accepted theory (Li et al., 2003; Donaldson et al., 2001; Bates et al., 2019). Oxidative stress occurs when the concentration of ROS (e.g., H_2O_2, •OH, $•O_2^-$) increases. Excessive ROS will break the balance of the oxidation-antioxidant system and induce inflammation that, in turn, can cause peroxidation on proteins or phospholipids, resulting in cell and tissue damage or death (Li et al., 2003; Baulig et al., 2003; Prahalad et al., 2001). ROS can be directly inhaled into the body by binding to particulate matter (particle-bound ROS) or catalyzed generation in vivo by stimulating cellular redox reactions through inhalation of components of PM (ROS-generation potential, OP). PM with higher OP tends to have more harmful health effects (He and Zhang, 2022; He et al., 2021; Crobeddu et al., 2017; Robinson, 2017; Weichenthal et al., 2016a). The OP reflects the $PM_{2.5}$ ROS generation capacity and could be used as a $PM_{2.5}$ cytotoxicity indicator.

The measurement method of OP can be divided into cellular analysis and acellular analysis. The cellular OP method can account for biological reactions involving ROS production and reflects the real situation of exposure in organisms (Landreman et al., 2008) However, cellular methods are less reproducible, making it difficult to achieve analysis with huge sample volumes, and the choice of cell type or cell line can significantly affect the OP results (He et al., 2020). Compared with the cellular method, the acellular method has the advantages of fast speed, easy operation, high reproducibility, and low cost. Common acellular assays include dithiothreitol assay (OP^{DTT}), ascorbic acid assay (OP^{AA}), glutathione detection (OP^{GSH}), and electron spin (or paramagnetic) resonance (OP^{ESR}). OP^{ESR} measures the generation of •OH via electron spin resonance, while OP^{DTT}, OP^{AA}, and OP^{GSH} measure the depletion rate of chemical proxies for cellular reductants (DTT) or antioxidants (AA, GSH) which is proportional to the generation rate of ROS. OP^{DTT} is the most widely used method currently available and has been shown to be closely associated with multiple health endpoints (Bates et al., 2015; Abrams et al., 2017; Fang et al., 2016). OP^{GSH} and OP^{AA} has also been associated with various health endpoints (Maikawa et al., 2016; Weichenthal et al., 2016b,c). Calas et al. (2017) emphasized the importance of simulated lung fluid (SLF) for assessing the OP of PM. Different acellular assays focused on different redox reactions. For example, the ESR assay was more sensitive to H_2O_2 and •OH (Bates et al., 2019), while the DTT assay was more sensitive to hydrogen peroxide (H_2O_2) and superoxide radical ($•O_2^-$) (Bates et al., 2019; Xiong et al., 2017). Some studies have used multi-OP methods to compensate for the specificity of a single probe for ROS response (Puthussery et al., 2020; Calas et al., 2018; H. Yu et al., 2021; Xu et al., 2021). Xu et al. (2021) used three probe methods (OP^{DTT}, OP^{AA}, OP^{GSH}) to estimate Canadian annual mean OP and found large differences in the sensitivity of the three methods to different components. Yu et al. (2018) demonstrated that HULIS, three transition metals (Fe, Mn, and Cu), and their interactions explain well the DTT depletion capacity of ambient PM, but the generation of •OH involves the contribution of other compounds (~50 %). Choosing multiple methods for OP measurement will certainly bring more comprehensive results, but it will also lead to a great increase of workload. So far, there is no consistent conclusion on the selection of OP methods, and it is essential to screen for an efficient and relatively comprehensive OP measurement system.

Various components of ambient $PM_{2.5}$ have been linked with OP (Verma et al., 2015a; Lyu et al., 2018; Wei et al., 2019) and quantifying the contribution of different components to OP has been the focus of research. Water-soluble fractions identified with ROS activity include HULIS (Verma et al., 2015a; Ma et al., 2019; Xu et al., 2020; Gonzalez et al., 2017; Huo et al., 2021), oxygenated quinones (Verma et al., 2015a; Lyu et al., 2018; Charrier and Anastasio, 2015), and water-soluble metals (Xu et al., 2021; Wei et al., 2019; Lin and Yu, 2020; Lin and Yu, 2019). Verma et al. (2015a) extracted HULIS of different polarities from $PM_{2.5}$ by multi-step fractionation to quantify their contribution to OP. In addition, Water-insoluble substances may also be a critical fraction of PM redox activity (McWhinney et al., 2013; Gao et al., 2017). McWhinney et al. (2013) reported that 89–98 % of the redox activity of diesel exhaust particles (DEPs) were water-insoluble. Jin et al. (2019) reported the decisive role of polycyclic aromatic hydrocarbons (PAHs) in the $PM_{2.5}$ OP in Beijing which resulted in a substantially higher per-mass $PM_{2.5}$ toxicity effect than in Guangzhou. Assessing the contribution of multi-component of ambient $PM_{2.5}$ to OP helps us to better understand the mechanisms of ROS generation. However, there are relatively few studies on the multi-component OP of ambient PM. The combination of multiple probes and multi-component (total, water-soluble, HULIS) for OP analysis is more limited, which is a great challenge in terms of workload alone.

A number of factors, including emission source (Verma et al., 2009; Kelly and Fussell, 2012; Al Hanai et al., 2019), secondary processes (Fang et al., 2017; Wei et al., 2022), meteorological conditions (Ming et al., 2017), could affect the chemical composition of ambient PM and further affect the PM OP. Highly time-resolved and long-term observations can usually collect more information on PM changes (emission sources or chemical composition), helping us better understand the driving factors influencing $PM_{2.5}$ OP and improving the reliability of statistical results (H. Yu et al., 2021; Yang et al., 2021; S. Yu et al., 2019; Jain et al., 2020). Jeong et al. (2020) conducted a 13-year (2004–2017) long-term ambient $PM_{2.5}$ sampling in Toronto and analyzed the interannual changes in emission sources and OPs. H. Yu et al. (2021) analyzed the OP of one-year $PM_{2.5}$ samples ($N = 241$) from five sampling sites in the Midwest region of the United States using OP^{AA}, OP^{GSH}, OP^{DTT}, and OP^{OH}, and found that most OP endpoints showed similar spatiotemporal trends across different sites and seasons. At present, the time resolution of most long-term observations is relatively low (H. Yu et al., 2021; Jeong et al., 2020; Borlaza et al., 2022), in which interannual and seasonal variability can be captured, while short-term pollution events and diurnal variation are ignored.

In this study, we take Shenzhen, a typical megacity city in the Pearl River Delta (PRD), as the research object to conduct a long-term analysis of the OP of $PM_{2.5}$. Based on multiple chemical probe methods (OP^{DTT}, OP^{GSH}, OP^{OH}), we attempt to quantitatively and comprehensively assess the OP of multi-components. Combined meteorological conditions and $PM_{2.5}$ chemical composition analysis, we also analyzed the seasonal and diurnal variations of OP and identified the components and sources that have a significant impact on the OP of $PM_{2.5}$ in Shenzhen.

2. Materials and methods

2.1. Sample collection and gravimetric analysis

Sampling was conducted on the rooftop of the administrative building of the Southern University of Science and Technology (22.604°N,114.006°E) in an urban area of Shenzhen from November 2020 to February 2021 (winter, 84 samples) and August 2021 to October 2021 (summer, 48 samples). Meteorological data during the sampling period were obtained from monitoring stations next to the sampling site. An XT-1025 high-volume intelligent sampler (XT1025, Shanghai XTrust Analytical Instruments Co., Ltd., China) with a flow rate of $1 m^3$/min was used to collect $PM_{2.5}$ samples on 8 × 10 in quartz filters (WhatmanQMA, 1851-865) for about 11 h (daytime is 07:30–19:00 local standard time (LST); nighttime is 19:30–06:00 LST of the next day). Detailed sampling information over the two seasons in Shenzhen is summarized in Table S1 of the supporting information (SI). All samples were collected on prebaked (500 °C for 5 h) quartz fiber filters; the $PM_{2.5}$-loaded filters were wrapped in aluminum foils and stored at −20 °C until analysis.

Before and after the collection, the filters were weighed under the constant temperature and humidity (22 ± 2 °C, 50 ± 2 %) for 48 h. Gravimetric analysis was conducted using a microbalance with an accuracy of 0.01 mg (MCE-C, Sartorius, Germany). Each filter was weighed at least three times, and the acceptable deviations among the repetitions were <5 × 10^{-4} g; the average of the readings was used for statistical analysis. All the resulting PM mass had been corrected by blanks. The $PM_{2.5}$ mass concentration was calculated using the weight difference divided by sampled air volume before and after sampling. Each $PM_{2.5}$-loaded filter was punched into small square pieces (1 cm^2) for subsequent chemical and OP analysis.

2.2. $PM_{2.5}$ extraction and chemical composition analysis

2.2.1. Multiple substances extraction

2.2.1.1. Total $PM_{2.5}$. $PM_{2.5}$-loaded filters were extracted via sonication for 40 min in deionized water (DI; Milli-Q; resistivity = 18.2 MΩ/cm) and used directly for subsequent OP analysis (Gao et al., 2017). The filter punch was also left in the extracts.

2.2.1.2. Water-soluble fraction extraction. $PM_{2.5}$-loaded filters were extracted via sonication for 40 min in deionized water; the sonicated solution was filtered through polytetrafluoroethylene membranes (0.22 μm) to remove insoluble particles, and the extracts were used for OP and water-soluble fraction chemical analysis.

2.2.1.3. HULIS fraction extraction. The segregation of HULIS was performed by a one-step solid phase extraction procedure, which has been applied in many studies (Huo et al., 2021; Lin and Yu, 2020; Fan et al., 2016). Briefly, 30 cm^2 filter samples were ultrasonically extracted with 25 ml of deionized water, and the extracted solutions were filtered with polytetrafluoroethylene (PTFE) membranes (0.22 μm) to remove solid impurities and filter debris. The pH value of the filtrate was adjusted to 2 with 2.4 M HCl and then introduced into a preconditioned solid-phase extraction cartridge (Oasis HLB, 30 mm, 60 mg/cartridge, Waters, USA). The SPE cartridge was prerinsed with two portions of 1 ml deionized water to remove soluble impurities. Finally, the remaining organics were eluted 4 times with 3 ml of methanol, and the eluate was evaporated to dryness under a gentle stream of nitrogen. The HULIS samples were redissolved in 20 ml of deionized water for the OP measurement.

2.2.2. Chemical composition analysis

The elemental and organic carbon content of the $PM_{2.5}$ was measured on a small section (0.5 cm^2) of the filters as per NIOSH (National Institute for Occupational Safety and Health) protocol (Birch and Cary, 1996) using a thermal/optical Carbon analyzer (DRI Model 2015). Nine water-soluble inorganic ions (SO_4^{2-}, NO_3^-, Cl^-, F^-, Na^+, NH_4^+, K^+, Ca^{2+}, and Mg^{2+}) were analyzed using Ion Chromatography (Dionex Aquion IC, Mexico); water-soluble organic carbon was measured using a Total Organic Carbon analyzer (TOC, Multi N/C 3100, Germany), and twelve typical water-soluble metals (V, Mn, Fe, Cu, Co, Ni, Ti, Cr, Zn, As, Cd, and Pb) were detected by Inductively Coupled Plasma Mass Spectrometer (ICP-MS, Thermo Fisher ICAP RQ). The extracts were acidified by HNO_3 (2 % final concentration) before analyzing the water-soluble metals; each sample was analyzed in three times. For every twelve samples, one filter blank solution was used as the control group, the relative standard deviations (RSD) for most metals were below 2 %, indicating good analytical precision.

2.3. Oxidative potential analysis

In this work, we used three different chemical probe methods to analyze the OP of various components of $PM_{2.5}$. Including OP^{DTT}, OP^{OH} and $OP^{GSH-SLF}$. The reaction mechanism is shown in Fig. S1. Each sample was analyzed three times. For every 12 samples, two parallel samples and one filter blank solution was used as the control group.

2.3.1. OP^{DTT} assay

OP^{DTT} is a commonly used chemical assay. In this study, the assay was modified from the DTT assay of H. Yu et al. (2019). Briefly, 3.5 ml of the sample, 1 ml of potassium phosphate buffer (K-PB, pH ~ 7.4, Chelex resin-treated), and 0.5 ml of 2 mM DTT were added to the reaction vial in a 37 °C water bath. At fixed time intervals (5, 15, 25, and 35 min), 500 μl of the reaction mixture was withdrawn and mixed with 0.5 ml of 0.2 mM DTNB, which forms a yellow-colored complex, 2-nitro-5-thiobenzoic acid (TNB); the absorbance of this complex was measured at a wavelength of 412 nm using a UV–visible spectrophotometer (T2600, Shanghai Yoke Instrument). Linear regression was applied to the data points measured at various time, and the slope was used to estimate the overall DTT consumption rate. Lin et al. (2022) reported a decaying DTT consumption rate with time due to the low DTT concentration and long reaction time. In this study, the average ratio of consumed DTT was 46.50 % ± 16.17 %. Hence, we achieved a strong linearity in OP^{DTT} (r_{mean} = −0.9933). Multiple field blanks and positive controls (9,10-phenanthraquinone) were also analyzed along with the samples.

2.3.2. OP^{OH} assay

We followed the procedure of Xiong et al. (2017) for the OP^{OH} experiments. Briefly, 3.5 ml of the sample, 1 ml of K-PB buffer, 2 ml of 60 mM Disodium terephthalate (TPT), and 1 ml of 1.2 mM DTT were added to the reaction vial and kept at a 37 °C water bath. TPT captures •OH and generates a fluorescent product, 2-hydroxyterephthalic acid (2-OHTA), with a yield of 35 % at pH = 7.4 (Li et al., 2019; Saran and Summer, 1999; Linxiang et al., 2004). At fixed time intervals (10, 20, 30, and 40 min), 200 μl of the reaction mixture was withdrawn and mixed with 0.5 ml of 100 mM DMSO (kept in a separate vial) to quench the •OH generation. The fluorescence intensity of 2-OHTA was measured three times by a Fluorescence Spectrophotometer (RF6000, SHIMADZU) at excitation/emission wavelengths of 310 nm/425 nm, and the mean value of the results was taken as the final concentration, respectively. The concentration of 2-OHTA was determined by calibrating the instrument with standards of known concentrations, and the generation rate of ·OH was calculated after dividing the formation rate of 2-OHTA by 0.35.

2.3.3. $OP^{GSH-SLF}$ assay

The $OP^{GSH-SLF}$ assay in this study largely followed the protocol of H. Yu et al. (2019). Briefly, 3.5 ml of the sample, 1 ml of 0.1 M K-PB, and 0.5 ml of SLF (concentrations of ascorbic acid (AA), L-ascorbic acid (GSH), uric acid (UA), and citric acid (CA) as 200 μM, 100 μM, 100 μM, and 300 μM) were added to the reaction vial and kept at 37 °C water bath (Charrier and Anastasio, 2015; Charrier et al., 2014). At fixed time intervals (5, 15, 25, and 35 min), 400 μl of the reaction mixture was withdrawn and mixed with 1.6 ml of 2 mM OPA, which forms a fluorescent product (GS-OPA) (Godri et al., 2011; Bohmer et al., 2011). It can be detected by a Fluorescence Spectrophotometer (RF6000, SHIMADZU). The fluorescence intensity was measured three times at the excitation/emission wavelength of 310 nm/427 nm. The mean value of the results was taken as the final concentration of GS-OPA.

The final OP measure was blank-corrected and normalized by the volume of sampled air (OP_v, units of μmol/min/m^3). The mass-normalized OP (OP_m) was further obtained by dividing the OP_v by the particle mass concentration (expressed in μmol/min/μg). OP_v is useful for toxicological and epidemiologic studies, while OP_m is more relevant for comparing OP of PM with different compositions (Bates et al., 2019).

2.4. Backward trajectory analysis with HYSPLIT

We modeled the origins and transport pathways of air masses arriving at the Shenzhen sampling site (22.604°N, 114.006°E) for 48 h backward trajectories using the HYSPLIT model version 4.0 provided by the National Oceanic and Atmospheric Administration (NOAA) Air Resources Laboratory (Wang et al., 2020). The backward trajectories of the air masses were

calculated with a height of 50 m above ground level and began at 06:00 LST and 19:00 LST each day during summer and winter.

3. Results and discussion

3.1. Comparison of OP measurements

DTT is used as a chemical substitute for biological reducing agents (adenine dinucleotide (NADH) and nicotinamide adenine dinucleotide phosphate (NADPH)) to reduce oxygen to superoxide anion ($\bullet O^{2-}$), and the rate of DTT consumption is proportional to the concentration of redox-active species in the PM sample. The GSH method measures the rate of depletion of antioxidants (GSH) in SLF (AA, GSH, UA, and CA) exposed to PM and is more indicative of realistic human PM exposure conditions. OP^{DTT} and $OP^{GSH-SLF}$ are widely used methods that have been shown to be associated with a variety of health endpoints (e.g., fractional exhaled nitric oxide (Maikawa et al., 2016), lung cancer mortality (Weichenthal et al., 2016b), myocardial infarction (Zhang et al., 2016), myocardial infarction (Weichenthal et al., 2016c), etc.). We believe that the combination of OP^{DTT} and $OP^{GSH-SLF}$ could be a good choice for comprehensive assessment of the PM OP.

Hydroxyl radical (•OH) is the most reactive and destructive of the ROS catalyzed by PM (Son et al., 2015; Tong et al., 2016). The redox-active species in PM eventually generate •OH via Fenton-like reactions, quinone autotrophic cycles, or organic hydroperoxide decomposition (Tong et al., 2016, 2018; Hwang et al., 2021). Son et al. (2015) developed a specific probe (disodium terephthalate, TPT) analysis method for the detection of •OH and the TPT probe was also applied to capture •OH in different systems. Xiong et al. (2017) applied the TPT probe to the DTT system (OP^{DTT-OH}) and found that DTT was more sensitive to H_2O_2 and $\bullet O_2^-$ but could not represent •OH production. Therefore, we plan to add OP^{DTT-OH} to our OP probes to further enhance the detection of •OH production.

Here, we employed the OP^{DTT}, OP^{OH}, and $OP^{GSH-SLF}$ to quantify the OP of total PM2.5 ($OP^{total-DTT}$, $OP^{total-OH}$, $OP^{total-GSH}$). Fig. 1a shows the time series of $OP_m^{total-DTT}$, $OP_m^{total-GSH}$, and $OP_m^{total-OH}$. $OP_m^{total-DTT}$ is highly correlated with $OP_m^{total-GSH}$ (Fig. S2a, $r = 0.77$), suggesting that they are in agreement in assessing the results of PM OP and might be driven by the same ROS-active species. There were large fluctuations in $PM_{2.5}$ mass concentrations during the sampling period. Huge differences in the ratio of each chemical component in $PM_{2.5}$ were also found in the subsequent analysis, which were caused by changes in emission sources or meteorological conditions. Nevertheless, $OP_m^{total-DTT}$ and $OP_m^{total-GSH}$ still showed such a strong correlation, indicating that the reducing abilities of DTT and GSH under PM exposure were comparable. However, the results of $OP_m^{total-DTT}$ and $OP_m^{total-OH}$ (Fig. 1a) differed dramatically. The OP_m^{OH} method was introduced to compensate for the inability of the DTT probe to accurately represent •OH. The difference between them might be caused by the drive of different ROS-active species. In the subsequent experiments, we demonstrated that OP_m^{DTT} is mainly influenced by OC and OP_m^{OH} is more dominated by heavy metals. Based on the above analysis, we believe that the combination of OP_m^{DTT} and OP_m^{OH} could be an effective way to comprehensively assess the OP of PM.

3.2. OP of total $PM_{2.5}$, water-soluble, and HULIS

In addition to the OP of the total $PM_{2.5}$, we also measured the OP of the water-soluble fraction (OP^{WS-DTT}, OP^{WS-OH}) and the HULIS fraction ($OP^{HULIS-DTT}$, $OP^{HULIS-OH}$). Water-soluble fractions have been considered the main contributors to the OP of $PM_{2.5}$ (Wang et al., 2020; Verma et al., 2014; Cheng et al., 2021; Verma et al., 2015b), including water-soluble heavy metals, oxygenated quinones, and HULIS, all of which have been shown to have significant OP activities (Verma et al., 2015a; Lyu et al., 2018; Gonzalez et al., 2017; Charrier and Anastasio, 2015; Lin and Yu, 2011). We extracted the water-soluble fractions and HULIS fractions separately to quantify their contribution to the total $PM_{2.5}$ OP.

3.2.1. Total $PM_{2.5}$ versus water-soluble extracts

Fig. 1b and c show the time series of $OP_m^{total-DTT}$ and OP_m^{WS-DTT}, $OP_m^{total-OH}$ and OP_m^{WS-OH}, respectively. OP_m^{WS-DTT} and $OP_m^{total-DTT}$ showed almost the same value (Fig. S2b, $r = 0.90$), indicating that the water-insoluble components of ambient $PM_{2.5}$ in Shenzhen may have little contribution to OP. OP_m^{WS-OH} and $OP_m^{total-OH}$ also have a significant correlation (Fig. S2c, $r = 0.86$), but different from the DTT assay. The OP_m^{WS-OH} value is significantly higher than $OP_m^{total-OH}$ value. Part of the generated •OH might

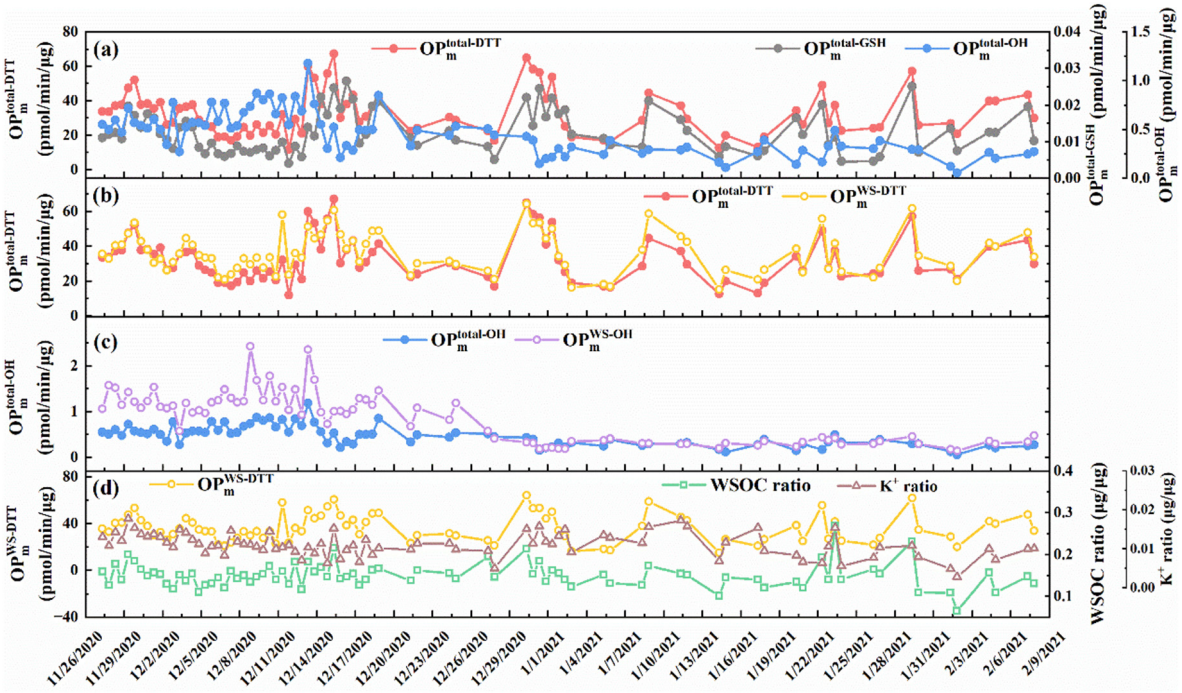

Fig. 1. The time series of (a) $OP_m^{total-DTT}$, $OP_m^{total-GSH}$, and $OP^{total-OH}$; (b) $OP_m^{total-DTT}$ and OP_m^{WS-DTT}; (c) $OP_m^{total-OH}$ and OP_m^{WS-OH} (d) OP_m^{WS-DTT}, WSOC ratio and K^+ ratio during the winter sampling period.

combine with the non-soluble PM surface or residual quartz filter to form surface-bound •OH rather than free in solution (Khachatryan et al., 2011; Khachatryan and Dellinger, 2011), which reduced the capture efficiency of TPT. Our follow-up research will mainly focus on the analysis of water-soluble fraction by the OP^{DTT} and OP^{OH}.

3.2.2. WS extracts versus HULIS extracts

HULIS is the hydrophobic fraction of the water-soluble organic (WSOC) fraction in the ambient $PM_{2.5}$, accounting for more than half of the total WSOC (Huo et al., 2021). The HULIS fraction is generally considered to be related to OP (Verma et al., 2015a; Ma et al., 2019; Xu et al., 2020; Gonzalez et al., 2017). We separated the HULIS from the water-soluble fraction to exclude the interference of other components such as heavy metals to observe the HULIS contribution to the OP. Fig. 2 shows the comparison between the OP^{DTT} and OP^{OH} results of the water-soluble and HULIS fraction in winter and summer samples, respectively.

For winter samples, the mean $OP_m^{HULIS-DTT}$ (10.25 pmol/min/μg) was approximately 28.34 % of the mean OP_m^{WS-DTT} (36.16 pmol/min/μg) and shows a strong correlation in winter (Fig. S3a, $r = 0.69$), indicating that the HULIS component might be critical in determining the OP^{DTT} for winter samples. OP_m^{WS-OH} and $OP_m^{HULIS-OH}$ show completely different results; The HULIS fraction, which was segregated from the water-soluble fraction of ambient $PM_{2.5}$, had almost negligible activity in $OP_m^{HULIS-OH}$ (Fig. 2b). The HULIS fraction of the winter samples may not contribute to OP_m^{OH} (Fig. S3b, $r = -0.26$), or only provide a certain catalytic or synergistic effect (Yu et al., 2018).

For summer samples, the water-soluble fraction and the HULIS fraction of OP^{DTT} and OP^{OH} of summer samples all showed significant but not strong correlation (Fig. S3c, $r = 0.34$, $p < 0.05$; Fig. S3d, $r = 0.39$, $p < 0.01$), and HULIS may have a partial contribution to both OP^{DTT} and OP^{OH}. Meanwhile, we find two patterns in summer, OP_m^{WS-DTT} in August ($OP_m{}^{WS-DTT}{}_{mean} = 38.52$ pmol/min/μg) was substantially higher than in September and October ($OP_m{}^{WS-DTT}{}_{mean} = 18.45$ pmol/min/μg). Therefore, our subsequent analysis will discuss these two periods separately. $OP_m^{HULIS-DTT}$ accounted for about 13.71 % of OP_m^{WS-DTT} in August ($OP_m{}^{HULIS-DTT}{}_{mean} = 5.28$ pmol/min/μg) and approximately 29.59 % in September and October ($OP_m{}^{HULIS-DTT}{}_{mean} = 5.46$ pmol/min/μg). We believe that OP_m^{WS-DTT} in August was dominated by heavy metals, thus causing such a large difference between OP_m^{WS-DTT} and $OP_m^{HULIS-DTT}$, while in September and October, heavy metals and HULIS together affected the OP_m^{WS-DTT}. The OP_m^{WS-OH} in summer was similar to those in winter, and the HULIS had little contribution to OP_m^{WS-OH}(Fig. 2b), which might be driven by heavy metals.

3.3. $PM_{2.5}$ and chemical composition

Fig. S4a shows the mean, median, and interquartile range of $PM_{2.5}$, EC, OC, WSOC, and OC/EC ratio analyzed from PM samples collected in our study. The mean values of $PM_{2.5}$, OC, EC, WSOC, and OC/EC in winter were all higher than those in summer (Table S2). The $PM_{2.5}$ concentration varies greatly in winter, and pollution events occur more frequently (Fig. S4a). The $PM_{2.5}$ concentration in summer was generally low, especially in August ($PM_{2.5mean} = 20.39$ μg/m^3), which was substantially lower than that in September ($PM_{2.5mean} = 40.19$ μg/m^3) and October ($PM_{2.5mean} = 32.42$ μg/m^3). The Asian monsoon influences the synoptic-scale meteorology of the PRD. In winter, the north and northeast winds prevailed (Fig. S5a, b), and the $PM_{2.5}$ could be influenced by the inland ambient pollutants via long-distance transport. In summer, the Asian monsoon brings clean and humid air over the South China Sea (Fig. S5c, d, e) resulting in low $PM_{2.5}$ mass concentrations.

3.3.1. OC/EC ratio

The ratio of OC/EC is commonly used to estimate the relative contributions of primary and secondary sources (Zhang et al., 2011; Cao et al., 2006; Na et al., 2004). In typical urban areas, the primary OC/EC value is usually considered to be 2, derived from tunnel studies in urban areas (Mancilla et al., 2012; Zhu et al., 2010; Mancilla et al., 2015a; Hao et al., 2019). The minimum OC/EC values ($OC/EC_{min} = 2.51$) of ambient $PM_{2.5}$ samples are consistent with the characteristics of urban sources. The OC/EC value in both winter ($OC/EC_{mean} = 7.47$) and summer ($OC/EC_{mean} = 5.36$) were higher than the primary OC/EC. We followed the protocol of Mancilla et al. (2015b) to estimate the concentration of secondary organic carbon (SOC, $OC/EC_{prim} = 2$), as shown in Fig. S6. The results showed that SOC concentration was strongly correlated with ozone concentration (Fig. S6b, $r = 0.77$) in summer, the high oxidative atmospheric conditions were more conducive to secondary organic aerosols (SOA) formation (Yuan et al., 2018; Yang et al., 2022) ($SOC/OC_{mean} = 64.35$ %). On the contrary, the photochemical oxidation is not the leading cause of the elevated OC/EC ratio ($r = 0.47$) in winter, probably due to the influence of primary emissions from transported non-urban sources. Fig. 1d shows the time series of WSOC ratio and K^+ ratio for ambient $PM_{2.5}$ samples in winter. K^+ ratios and WSOC ratios show similar temporal trends (Fig. S2e, $r = 0.5$), and

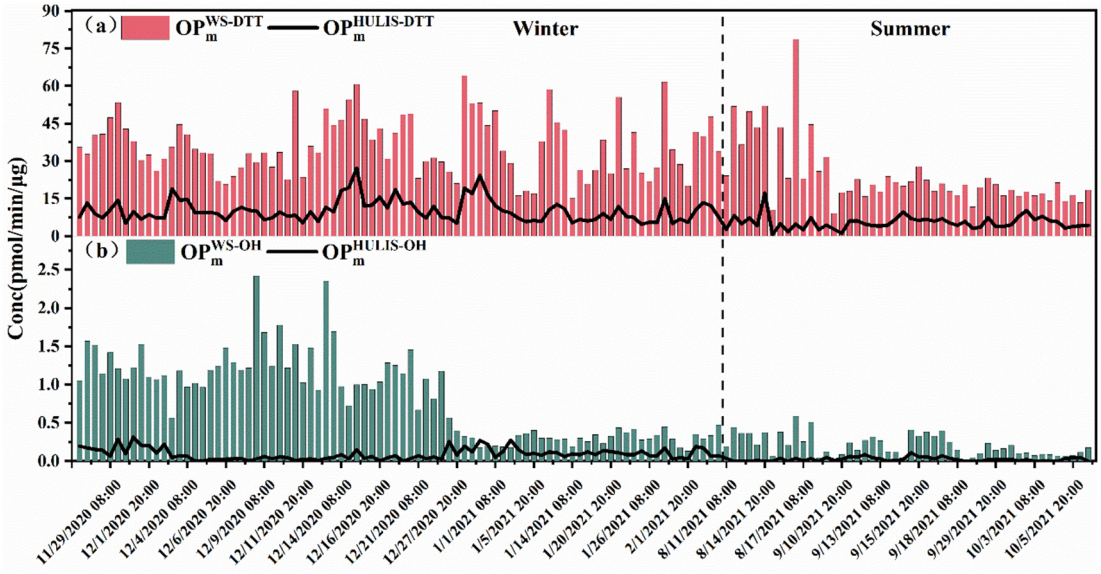

Fig. 2. Time series of (a) OP_m^{WS-DTT} vs $OP_m^{HULIS-DTT}$; (b) OP_m^{WS-OH} vs $OP_m^{HULIS-OH}$ during the winter (left of dash line, 8:00 for daytime samples, 20:00 for nighttime samples) and summer (right of dash line).

water-soluble K^+ is often regarded as a tracer for biomass burning (Pachon et al., 2013; Zong et al., 2016). Therefore, much of the WSOC in winter samples might come from the contribution of biomass burning. The biomass burning sources transported by long-distance transmission from the north significantly increase primary OC/EC ratios (typically biomass combustion OC/EC = 4 to 8), which leads to the use of OC/EC_{prim} = 2 seriously underestimating the percentage of primary organic aerosol (POA) in ambient $PM_{2.5}$.

3.3.2. Water-soluble metals

Fig. S4b shows the results of various water-soluble metals over 132 samples in winter and summer. Zn, Fe, Mn, and Cu were the most abundant metals (Zn_{mean} = 203.83 ng/m^3, 59.75 ng/m^3, Fe_{mean} = 64.19 ng/m^3, 31.68 ng/m^3, Mn_{mean} = 18.2 ng/m^3, 9.31 ng/m^3, and Cu_{mean} = 9.30 ng/m^3, 5.16 ng/m^3 in winter and summer, respectively), followed by Pb, Ti, As, Cr, Ni, and V. Cd and Co were in very low concentrations in both winter and summer (Table S2). Most metals show higher concentrations in winter than in summer, except for V (0.86 ng/m^3 in winter and 2.02 ng/m^3 in summer) and Ni (1.04 ng/m^3,1.74 ng/m^3). Note that V, Ni, and high V/Ni ratio are usually used as ship emissions traces (Agrawal et al., 2009; Zhang et al., 2019; Liu et al., 2017; G. Yu et al., 2021). Although G. Yu et al. (2021) found that stepwise marine fuel oil regulations resulted in a sharp decrease in ambient V concentration and V/Ni ratio in Shanghai, relatively high V concentration and V/Ni ratio can still be used as indicators of ship emissions. Summer $PM_{2.5}$ was significantly affected by the sea breeze (Fig. S5c, d), which leads to higher V concentrations and V/Ni ratios (V/Ni_{mean} = 1.16, 0.83 in winter and summer, respectively). The most abundant metals of Fe, Cu, and Mn, are generally considered to be ROS-active metals (Wei et al., 2019; Charrier and Anastasio, 2015; Fang et al., 2017; Charrier et al., 2014; Olechnowicz et al., 2018), the average mass concentration of Fe, Mn, and Cu in winter was about twice that in summer. Traffic emissions are considered to be the main source of heavy metals in PM, tire abrasion, lubricants, and the corrosion of vehicular parts lead to Fe, Cu, and Zn pollution (Duan and Tan, 2013; Hou et al., 2019). Industrial activities (e.g., power plants, mining activities, metal-smelting industry, and chemical plants) are the minor source of heavy metal pollution.

3.4. Relationship between $PM_{2.5}$ components and OP

3.4.1. $PM_{2.5}$ mass concentration and OP

Fig. 3a and b show the correlation between $PM_{2.5}$ mass concentration and OP in winter and summer, respectively. We observed negative correlations between $PM_{2.5}$ mass concentration and OP_m^{WS-DTT} in both winter and summer. When the $PM_{2.5}$ mass concentration was <30 μg/m^3, the OP_m^{WS-DTT} increased sharply with the decrease of $PM_{2.5}$ mass concentration. For OP_m^{WS-OH}, we observed a similar pattern only in summer when the $PM_{2.5}$ concentration was <30 μg/m^3. Some previous studies have reported similar trends. Xu et al. (2020) analyzed OP in Shanghai PM and found that samples with higher OP_m occurred when $PM_{2.5}$ concentrations were lower. Li et al. (2019) found a negative correlation between OP_m and $PM_{2.5}$ mass concentrations in Beijing and Wangdu, and the change rate of OP_m increased with the decrease of $PM_{2.5}$ mass concentration and is significantly slower in heavy pollution weather($PM_{2.5}$ mass concentration ≥ 75 μg/m^3). They attributed this negative correlation to SO_4^{2-}, NO^{3-}, and NH_4^+ dominating the increase of $PM_{2.5}$ mass concentrations, while these secondary inorganic components do not contribute to the generation of ROS. However, our results showed that the inorganic ion per unit mass concentrations (μg/μg $PM_{2.5}$) did not increase significantly with the increase of $PM_{2.5}$ mass concentration, which could not explain the sharp change trend of OP_m^{WS-DTT} we observed. We compared the trends of the per unit mass concentrations of other components in $PM_{2.5}$ and found that OC and SOC (Fig. 3c) in winter samples and OC, SOC, V, Ni, Fe, Na^+, and Mg^{2+} (Fig. 3d, e, f) in summer samples showed similar negative correlations with $PM_{2.5}$ mass concentrations. The K^+ ratio did not show a consistent negative correlation when the $PM_{2.5}$ mass concentration was <30 μg/m^3, suggesting that biomass burning source was not the dominant factor of OP during the low pollution period. SOC (r = −0.53) might be the main contributor to the low concentration of $PM_{2.5}$ OP_m^{WS-DTT} in winter. V, Ni, Na^+, and Mg^{2+} are typical indicators of marine sources (Agrawal et al., 2009; Zhang et al., 2019; Liu et al., 2017; G. Yu et al., 2021) (ship sources and sea salt), and ship emissions are also an important source of Fe. The summer period with $PM_{2.5}$ mass concentrations <30 μg/m^3 was more influenced by clean air masses from the South China Sea with ship emissions. The high ROS-active species contained in ship sources and atmospheric secondary oxidation processes enhance the $PM_{2.5}$ OP_m.

3.4.2. $PM_{2.5}$ components and OP

Table S3 shows the Pearson correlation coefficients between the two OP methods (OP^{DTT}, OP^{OH}) and $PM_{2.5}$ components. We observed unique patterns in August different from September and October, and we discuss August separately from the summer sample.

3.4.2.1. Winter. The OP_m^{WS-DTT} of winter samples showed a strong correlation with OC (r = 0.64), which was consistent with Samara (2017) and Shang et al. (2022); OP_m^{WS-OH} showed a medium correlation with Fe (r = 0.49). When we separated the HULIS fraction from the water-soluble fraction, the $OP_m^{HULIS-OH}$ activity was negligible (Fig. 2b), suggesting that heavy metals might dominate OP_m^{WS-OH}. Yu et al. (2018) confirmed the dominance of heavy metals such as Fe, Cu, and Mn for •OH generation by comparing the OP^{DTT} and OP^{OH} values of various ROS-active species. Besides, we found a strong correlation between OP_m^{WS-OH} and Zn (r = 0.63) as well. Zn is a non-redox active species with few contribution to OP (Charrier and Anastasio, 2012). Lovett et al. (1994) and Cheung et al. (2010) found a significant correlation between Zn and OP, and they attribute the association with OP to their collinearity with other same source substances. The sources of Zn in $PM_{2.5}$ mainly include waste incineration, steelmaking, vehicle emission, non-tailpipe emissions (rubber tire wear and lubricating oil) (Querol et al., 2006; Hjortenkrans et al., 2007; Aucélio et al., 2007).

Fig. 1d shows the time series of OP_m^{WS-DTT}, WSOC ratio, and K^+ ratio. During the winter sampling period. The temporal trends of $OP_m^{WS-DTT}$and WSOC ratio were similar (Fig. S2d, r = 0.57), suggesting that DTT was WSOC-driven in winter. We have discussed in Section 3.3 that biomass burning from long-range transport in the north dominates the trend of WSOC in the winter samples. Therefore, the OP_m^{WS-DTT} of $PM_{2.5}$ in Shenzhen winter might be dominated by the long-distance transported biomass burning from the north.

3.4.2.2. August. Strong correlations were found among OP_m^{WS-DTT}, OP_m^{WS-OH}, OC, WSOC, metals, and most ions of the August samples (Fig. S7c), which indicates that there were unified emission sources for these components. V and Ni are typical tracers for ship sources (Zhang et al., 2019; G. Yu et al., 2021). The mass concentrations of V and Ni in August samples (V_{mean} = 2.20 ng/m^3, Ni_{mean} = 2.00 ng/m^3, V/Ni = 1.10) were substantially higher than those in winter (V_{mean} = 0.86 ng/m^3, Ni_{mean} = 1.04 ng/m^3). The masses of V and Ni per unit mass of $PM_{2.5}$ were also higher in August (V_{mean} = 0.16 ng/μg, Ni_{mean} = 0.15 ng/μg) than in winter (V_{mean} = 0.02 ng/μg, Ni_{mean} = 0.03 ng/μg). Therefore, ship emissions likely dominated both $PM_{2.5}$ mass concentration and OP in August.

3.4.2.3. September and October. In September and October, both OP_m^{WS-DTT} and OP_m^{WS-OH} showed strong correlation with WSOC (r = 0.51, r = 0.88), and Mn (r = 0.46, r = 0.73); OP_m^{WS-OH} was also strong correlated with Cu (r = 0.71), and Fe (r = 0.53), which indicated that the OP_m in the September and October samples might be affected by both metals and organics. Combining with the results of the HULIS fraction in Section 3.2.2, we believe that OP_m^{WS-OH} was dominated by metals in September and October, and OP_m^{WS-DTT} was affected by both metals and organics. While OP_m shows good correlations with a variety of metals (such as Zn, Pb, Cr, Cd, As), there are extremely high correlations among the metals themselves, and these correlations can be attributed to collinearity with Fe, and Mn, which are widely considered to be ROS-active metals. The mass

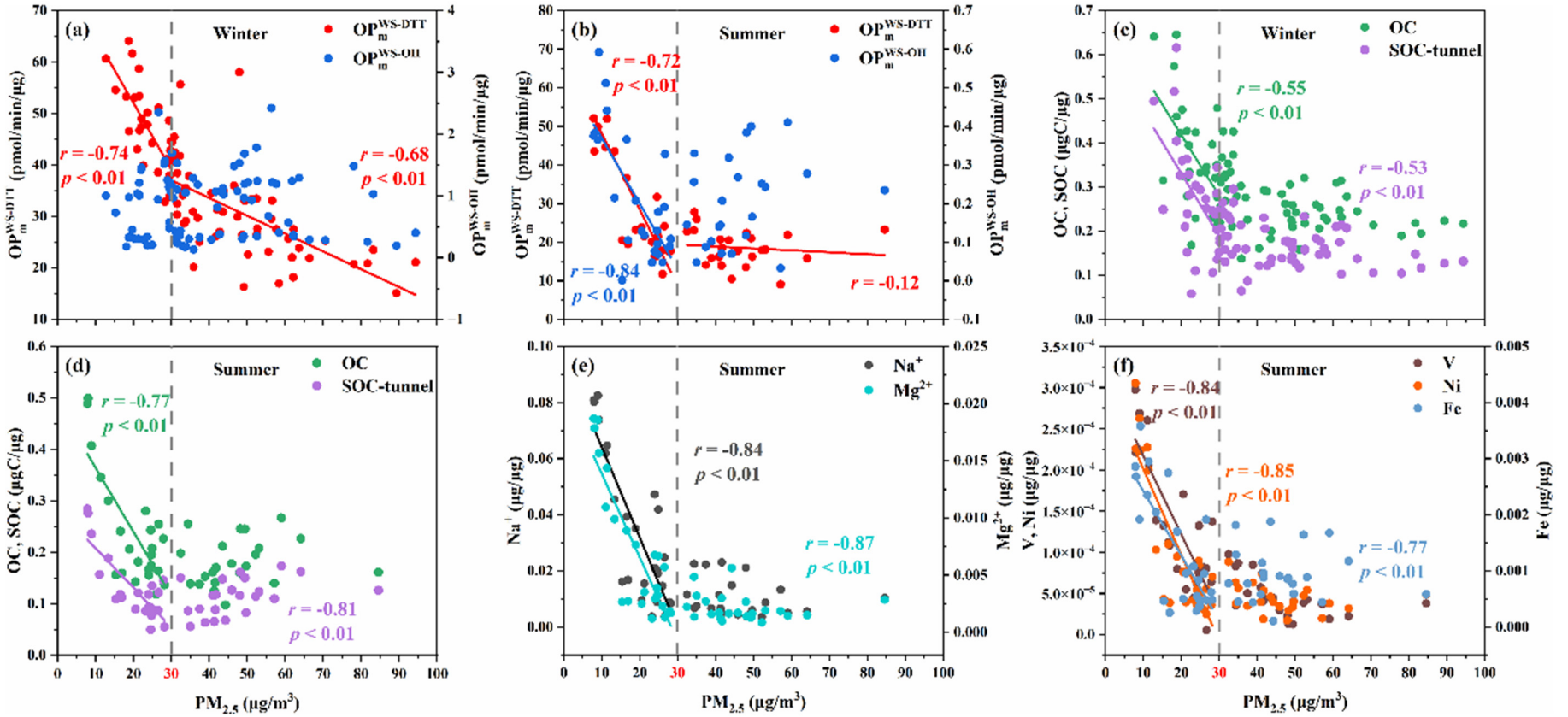

Fig. 3. Comparison between the ambient $PM_{2.5}$ mass concentration with (a) OP_m^{WS-DTT} and OP_m^{WS-OH} in winter; (b) OP_m^{WS-DTT} and OP_m^{WS-OH} in summer; (c) OC in winter; (d) OC and SOC in summer; (e) Na^+ and Mg^{2+} in summer; (f) V, Ni, and Fe in summer; the dash line represents the $PM_{2.5}$ mass concentration of 30 μg/m^3.

concentrations of V and Ni in September and October (V_{mean} = 1.94 ng/m^3, Ni_{mean} = 1.64 ng/m^3) were comparable to those in August, while the per unit mass concentrations of V and Ni (V_{mean} = 0.06 ng/μg, Ni_{mean} = 0.04 ng/μg) were much lower than those in August, indicating that ship sources accounted for a higher percentage in August than in September and October, this is probably the main reason for the higher OP_m^{WS-DTT} in August.

3.5. Seasonal and diurnal variation of OP

Long-term and high-resolution $PM_{2.5}$ observations allow us to observe seasonal and diurnal variations in OP. OP_m^{WS-DTT} and OP_m^{WS-OH} showed the same seasonal variation pattern, which was much higher in winter than in summer (Table S2). The OP_m^{WS-DTT} and OP_m^{WS-OH} in winter were about 1.5 and 4 times that in summer, respectively. The change in the prevailing monsoon in winter (north and northeast winds) and summer (south and southeast winds) caused a difference in the external source. Winter was significantly influenced by biomass burning sources transmitted from the north, while summer was mainly dominated by ship sources. Biomass burning sources have high toxicity and human health risks (Wu et al., 2022).

Fig. S8 shows the diurnal variations of OP_m^{WS-DTT} and OP_m^{WS-OH} in winter and summer. We did not find significant diurnal variation in OP in the winter samples (Fig. S8a, b), and the winter $PM_{2.5}$ OP was mainly influenced by biomass burning sources with long-range transport, and such long-range transport sources usually do not have a diurnal variation trend. For the summer samples (Fig. S8c, d), we observed a regular diurnal variation (nighttime > daytime) in OP_m^{WS-DTT}, especially in August, when the nighttime OP_m^{WS-DTT} was even more than twice as high as the daytime OP_m^{WS-DTT}. Similar diurnal variation was observed by OP_m^{WS-OH} only in August. Given the strong correlation between most of the components (Na, V, and Ni, etc.) in August (Fig. S7c), and at the same time showing a consistent diurnal variation pattern (Fig. S9, nighttime > daytime). We attribute the diurnal variation in August to the influence of emission sources (ship emission dominated). The higher temporal resolution helps us to identify the contribution of specific emission sources to the OP.

4. Conclusions

In this study, we carried out a long-term analysis of the OP of 132 ambient $PM_{2.5}$ samples in Shenzhen based on multi-component and multi-probe assays. Comparing the OP results of multi-probe assays, we found that using both OP^{DTT} and OP^{OH} could lead to effective and comprehensive results. Although previous studies (Xiong et al., 2017) reported the insensitivity of the DTT method to •OH, this is the first demonstration for large number of ambient environmental sample. This study also reveals different driving factors of OP in winter and summer in Shenzhen. Winter usually had higher $PM_{2.5}$ mass concentrations, and the long-range transported pollutants from the north such as biomass burning emissions, causing the elevated OP. The change in monsoon made the summer mainly influenced by marine sources, and ship emissions dominated the OP. The monsoonal climate in the PRD region caused distinct external source influences in winter and summer, which was further reflected in the components and OPs. In addition, we found a significant negative correlation between $PM_{2.5}$ mass concentration and OP. Our work demonstrates that the OP of ambient $PM_{2.5}$ was sensitive to the changes in meteorological condition, emission source, and atmospheric secondary process, which requires multi-method, multi-component and long-term investigations.

CRediT authorship contribution statement

Chunbo Xing: Methodology, Data analysis, Visualization, Writing - original draft, Writing - review & editing. **Yixiang Wang**: Writing - review & editing. **Xin Yang**: Funding acquisition, Supervision, Project administration, Resources, Writing - review & editing. **Yaling Zeng**: Investigation. **Jinghao Zhai**: Investigation. **Baohua Cai**: Investigation. **Antai Zhang**: Investigation. **Tzung-May Fu**: Investigation. **Lei Zhu**: Investigation. **Ying Li**: Data curation, Resources. **Xinming Wang**: Resources. **Yanli Zhang**: Resources.

Data availability

Data will be made available on request.

Declaration of competing interest

The authors declare that they have no known competing financial interests or personal relationships that could have appeared to influence the work reported in this paper.

Acknowledgments

This work was supported by the Key Area Research and Development Program of Guangdong Provincial (2020B1111360001), Guangdong Provincial Observation and Research Station for Coastal Atmosphere and Climate of the Greater Bay Area (2021B1212050024), Shenzhen Science and Technology Program (KQTD20210811090048025) and National Natural Science Foundation of China (41827804, 42107119).

Appendix A. Supplementary data

Detailed descriptions of chemicals, sampling information, composition information, correlation analysis, backward trajectories, diurnal variation, seasonal variation, SOC, and time series of each component (Tables S1–S3, Figs. S1–S9). Supplementary data to this article can be found online at https://doi.org/10.1016/j.scitotenv.2022.160771.

References

Abrams, J.Y., Weber, R.J., Klein, M., Sarnat, S.E., Chang, H.H., Strickland, M.J., Verma, V., Fang, T., Bates, J.T., Mulholland, J.A., et al., 2017. Associations between ambient fine particulate oxidative potential and cardiorespiratory emergency department visits. Environ. Health Perspect. 125 (10), 107008. https://doi.org/10.1289/EHP1545.

Agrawal, H., Eden, R., Zhang, X., Fine, P.M., Katzenstein, A., Miller, J.W., Ospital, J., Teffera, S., Cocker III, D.R., 2009. Primary particulate matter from ocean-going engines in the Southern California Air Basin. Environ. Sci. Technol. 43 (14), 5398–5402.

Al Hanai, A.H., Antkiewicz, D.S., Hemming, J.D.C., Shafer, M.M., Lai, A.M., Arhami, M., Hosseini, V., Schauer, J.J., 2019. Seasonal variations in the oxidative stress and inflammatory potential of PM2.5 in Tehran using an alveolar macrophage model; the role of chemical composition and sources. Environ. Int. 123, 417–427. https://doi.org/10.1016/j.envint.2018.12.023.

Aucélio, R.Q., de Souza, R.M., de Campos, R.C., Miekeley, N., da Silveira, C.L.P., 2007. The determination of trace metals in lubricating oils by atomic spectrometry. Spectrochim. Acta B At. Spectrosc. 62 (9), 952–961. https://doi.org/10.1016/j.sab.2007.05.003.

Bates, J.T., Weber, R.J., Abrams, J., Verma, V., Fang, T., Klein, M., Strickland, M.J., Sarnat, S.E., Chang, H.H., Mulholland, J.A., et al., 2015. Reactive oxygen species generation linked to sources of atmospheric particulate matter and cardiorespiratory effects. Environ. Sci. Technol. 49 (22), 13605–13612. https://doi.org/10.1021/acs.est.5b02967.

Bates, J.T., Fang, T., Verma, V., Zeng, L., Weber, R.J., Tolbert, P.E., Abrams, J.Y., Sarnat, S.E., Klein, M., Mulholland, J.A., et al., 2019. Review of acellular assays of ambient particulate matter oxidative potential: methods and relationships with composition, sources, and health effects. Environ. Sci. Technol. 53 (8), 4003–4019. https://doi.org/10.1021/acs.est.8b03430.

Baulig, A., Garlatti, M., Bonvallot, V., Marchand, A., Barouki, R., Marano, F., Baeza-Squiban, A., 2003. Involvement of reactive oxygen species in the metabolic pathways triggered by diesel exhaust particles in human airway epithelial cells. Am. J. Phys. Lung Cell. Mol. Phys. 285 (3), L671–L679.

Birch, M.E., Cary, R.A., 1996. Elemental carbon-based method for monitoring occupational exposures to particulate diesel exhaust. Aerosol Sci. Technol. 25 (3), 221–241. https://doi.org/10.1080/02786829608965393.

Bohmer, A., Jordan, J., Tsikas, D., 2011. High-performance liquid chromatography ultraviolet assay for human erythrocytic catalase activity by measuring glutathione as o-phthalaldehyde derivative. Anal. Biochem. 410 (2), 296–303. https://doi.org/10.1016/j.ab.2010.11.026.

Borlaza, L.J., Weber, S., Marsal, A., Uzu, G., Jacob, V., Besombes, J.-L., Chatain, M., Conil, S., Jaffrezo, J.-L., 2022. Nine-year trends of PM10 sources and oxidative potential in a rural background site in France. Atmos. Chem. Phys. 22 (13), 8701–8723. https://doi.org/10.5194/acp-22-8701-2022.

Calas, A., Uzu, G., Martins, J.M.F., Voisin, D., Spadini, L., Lacroix, T., Jaffrezo, J.L., 2017. The importance of simulated lung fluid (SLF) extractions for a more relevant evaluation of the oxidative potential of particulate matter. Sci. Rep. 7 (1), 11617. https://doi.org/10.1038/s41598-017-11979-3.

Calas, A., Uzu, G., Kelly, F.J., Houdier, S., Martins, J.M.F., Thomas, F., Molton, F., Charron, A., Dunster, C., Oliete, A., et al., 2018. Comparison between five acellular oxidative potential measurement assays performed with detailed chemistry on PM10 samples from the city of Chamonix (France). Atmos. Chem. Phys. 18 (11), 7863–7875. https://doi.org/10.5194/acp-18-7863-2018.

Cao, G., Zhang, X., Zheng, F., 2006. Inventory of black carbon and organic carbon emissions from China. Atmos. Environ. 40 (34), 6516–6527.

Charrier, J.G., Anastasio, C., 2012. On dithiothreitol (DTT) as a measure of oxidative potential for ambient particles: evidence for the importance of soluble transition metals. Atmos. Chem. Phys. 12 (19), 9321–9333. https://doi.org/10.5194/acp-12-9321-2012.

Charrier, J.G., Anastasio, C., 2015. Rates of hydroxyl radical production from transition metals and quinones in a surrogate lung fluid. Environ. Sci. Technol. 49 (15), 9317–9325. https://doi.org/10.1021/acs.est.5b01606.

Charrier, J.G., McFall, A.S., Richards-Henderson, N.K., Anastasio, C., 2014. Hydrogen peroxide formation in a surrogate lung fluid by transition metals and quinones present in particulate matter. Environ. Sci. Technol. 48 (12), 7010–7017. https://doi.org/10.1021/es501011w.

Cheng, Y., Ma, Y., Dong, B., Qiu, X., Hu, D., 2021. Pollutants from primary sources dominate the oxidative potential of water-soluble PM2.5 in Hong Kong in terms of dithiothreitol (DTT) consumption and hydroxyl radical production. J. Hazard. Mater. 405, 124218. https://doi.org/10.1016/j.jhazmat.2020.124218.

Cheung, K.L., Ntziachristos, L., Tzamkiozis, T., Schauer, J.J., Samaras, Z., Moore, K.F., Sioutas, C., 2010. Emissions of particulate trace elements, metals and organic species from gasoline, diesel, and biodiesel passenger vehicles and their relation to oxidative potential. Aerosol Sci. Technol. 44 (7), 500–513. https://doi.org/10.1080/02786821003758294.

Crobeddu, B., Aragao-Santiago, L., Bui, L.C., Boland, S., Baeza Squiban, A., 2017. Oxidative potential of particulate matter 2.5 as predictive indicator of cellular stress. Environ. Pollut. 230, 125–133. https://doi.org/10.1016/j.envpol.2017.06.051.

Crobeddu, B., Baudrimont, I., Deweirdt, J., Sciare, J., Badel, A., Camproux, A.C., Bui, L.C., Baeza-Squiban, A., 2020. Lung antioxidant depletion: a predictive indicator of cellular stress induced by ambient fine particles. Environ. Sci. Technol. 54 (4), 2360–2369. https://doi.org/10.1021/acs.est.9b05990.

Donaldson, K., Stone, V., Seaton, A., MacNee, W., 2001. Ambient particle inhalation and the cardiovascular system: potential mechanisms. Environ. Health Perspect. 109 (Suppl. 4), 523–527.

Duan, J., Tan, J., 2013. Atmospheric heavy metals and arsenic in China: situation, sources and control policies. Atmos. Environ. 74, 93–101. https://doi.org/10.1016/j.atmosenv.2013.03.031.

Fan, X., Wei, S., Zhu, M., Song, J., Peng, P.a., 2016. Comprehensive characterization of humic-like substances in smoke PM2.5 emitted from the combustion of biomass materials and fossil fuels. Atmos. Chem. Phys. 16 (20), 13321–13340. https://doi.org/10.5194/acp-16-13321-2016.

Fang, T., Verma, V., Bates, J.T., Abrams, J., Klein, M., Strickland, M.J., Sarnat, S.E., Chang, H.H., Mulholland, J.A., Tolbert, P.E., et al., 2016. Oxidative potential of ambient water-soluble PM2.5 in the southeastern United States: contrasts in sources and health associations between ascorbic acid (AA) and dithiothreitol (DTT) assays. Atmos. Chem. Phys. 16 (6), 3865–3879. https://doi.org/10.5194/acp-16-3865-2016.

Fang, T., Guo, H., Zeng, L., Verma, V., Nenes, A., Weber, R.J., 2017. Highly acidic ambient particles, soluble metals, and oxidative potential: a link between sulfate and aerosol toxicity. Environ. Sci. Technol. 51 (5), 2611–2620. https://doi.org/10.1021/acs.est.6b06151.

Gao, D., Fang, T., Verma, V., Zeng, L., Weber, R.J., 2017. A method for measuring total aerosol oxidative potential (OP) with the dithiothreitol (DTT) assay and comparisons between an urban and roadside site of water-soluble and total OP. Atmos. Meas. Tech. 10 (8), 2821–2835. https://doi.org/10.5194/amt-10-2821-2017.

Godri, K.J., Harrison, R.M., Evans, T., Baker, T., Dunster, C., Mudway, I.S., Kelly, F.J., 2011. Increased oxidative burden associated with traffic component of ambient particulate matter at roadside and urban background schools sites in London. PLoS One 6 (7), e21961. https://doi.org/10.1371/journal.pone.0021961.

Gonzalez, D.H., Cala, C.K., Peng, Q., Paulson, S.E., 2017. HULIS enhancement of hydroxyl radical formation from Fe(II): kinetics of fulvic acid-Fe(II) complexes in the presence of lung antioxidants. Environ. Sci. Technol. 51 (13), 7676–7685. https://doi.org/10.1021/acs.est.7b01299.

Hao, Y., Deng, S., Yang, Y., Song, W., Tong, H., Qiu, Z., 2019. Chemical composition of particulate matter from traffic emissions in a road tunnel in Xi'an,China. Aerosol Air Qual. Res. 19 (2), 234–246. https://doi.org/10.4209/aaqr.2018.04.0131.

He, L., Zhang, J., 2022. Particulate matter (PM) oxidative potential: measurement methods and links to PM physicochemical characteristics and health effects. Crit. Rev. Environ. Sci. Technol., 1–21 https://doi.org/10.1080/10643389.2022.2050148.

He, L.C., Cui, X.X., Li, Z., Teng, Y.B., Barkjohn, K.K., Norris, C., Fang, L., Lin, L.L., Wang, Q., Zhou, X.J., et al., 2020. Malondialdehyde in nasal fluid: a biomarker for monitoring asthma control in relation to air pollution exposure. Environ. Sci. Technol. 54 (18), 11405–11413. https://doi.org/10.1021/acs.est.0c02558.

He, L., Norris, C., Cui, X., Li, Z., Barkjohn, K.K., Brehmer, C., Teng, Y., Fang, L., Lin, L., Wang, Q., et al., 2021. Personal exposure to PM2.5 oxidative potential in association with pulmonary pathophysiologic outcomes in children with asthma. Environ. Sci. Technol. 55 (5), 3101–3111. https://doi.org/10.1021/acs.est.0c06114.

Hjortenkrans, D.S.T., Bergback, B., Haggerud, A., 2007. Metal emissions from brake linings and tires: case studies of Stockholm, Sweden 1995/1998 and 2005.

Hou, S., Zheng, N., Tang, L., Ji, X., Li, Y., Hua, X., 2019. Pollution characteristics, sources, and health risk assessment of human exposure to Cu, Zn, Cd and Pb pollution in urban street dust across China between 2009 and 2018. Environ. Int. 128, 430–437. https://doi.org/10.1016/j.envint.2019.04.046.

Huo, Y., Guo, Z., Li, Q., Wu, D., Ding, X., Liu, A., Huang, D., Qiu, G., Wu, M., Zhao, Z., et al., 2021. Chemical fingerprinting of HULIS in particulate matters emitted from residential coal and biomass combustion. Environ. Sci. Technol. 55 (6), 3593–3603. https://doi.org/10.1021/acs.est.0c08518.

Hwang, B., Fang, T., Pham, R., Wei, J., Gronstal, S., Lopez, B., Frederickson, C., Galeazzo, T., Wang, X., Jung, H., et al., 2021. Environmentally persistent free radicals, reactive oxygen species generation, and oxidative potential of highway PM2.5. ACS Earth Space Chem. 5 (8), 1865–1875. https://doi.org/10.1021/acsearthspacechem.1c00135.

Jain, S., Sharma, S.K., Vijayan, N., Mandal, T.K., 2020. Seasonal characteristics of aerosols (PM2.5 and PM10) and their source apportionment using PMF: a four year study over Delhi, India. Environ. Pollut. 262, 114337. https://doi.org/10.1016/j.envpol.2020.114337.

Jeong, C.-H., Traub, A., Huang, A., Hilker, N., Wang, J.M., Herod, D., Dabek-Zlotorzynska, E., Celo, V., Evans, G.J., 2020. Long-term analysis of PM2.5 from 2004 to 2017 in Toronto: composition, sources, and oxidative potential. Environ. Pollut. 263. https://doi.org/10.1016/j.envpol.2020.114652.

Jin, L., Xie, J., Wong, C.K.C., Chan, S.K.Y., Abbaszade, G., Schnelle-Kreis, J., Zimmermann, R., Li, J., Zhang, G., Fu, P., et al., 2019. Contributions of city-specific fine particulate matter (PM(2.5)) to differential in vitro oxidative stress and toxicity implications between Beijing and Guangzhou of China. Environ. Sci. Technol. 53 (5), 2881–2891. https://doi.org/10.1021/acs.est.9b00449.

Kelly, F.J., Fussell, J.C., 2012. Size, source and chemical composition as determinants of toxicity attributable to ambient particulate matter. Atmos. Environ. 60, 504–526. https://doi.org/10.1016/j.atmosenv.2012.06.039.

Khachatryan, L., Dellinger, B., 2011. Environmentally persistent free radicals (EPFRs)-2. Are free hydroxyl radicals generated in aqueous solutions? Environ. Sci. Technol. 45 (21), 9232–9239. https://doi.org/10.1021/es201702q.

Khachatryan, L., Vejerano, E., Lomnicki, S., Dellinger, B., 2011. Environmentally persistent free radicals (EPFRs). 1. Generation of reactive oxygen species in aqueous solutions. Environ. Sci. Technol. 45 (19), 8559–8566. https://doi.org/10.1021/es201309c.

Landreman, A.P., Shafer, M.M., Hemming, J.C., Hannigan, M.P., Schauer, J.J., 2008. A macrophage-based method for the assessment of the reactive oxygen species (ROS) activity of atmospheric particulate matter (PM) and application to routine (Daily-24 h) aerosol monitoring studies. Aerosol Sci. Technol. 42 (0278–6826), 946–957. https://doi.org/10.1080/02786820802363819.

Li, N., Sioutas, C., Cho, A., Schmitz, D., Misra, C., Sempf, J., Wang, M., Oberley, T., Froines, J., Nel, A., 2003. Ultrafine particulate pollutants induce oxidative stress and mitochondrial damage. Environ. Health Perspect. 111 (4), 455–460. https://doi.org/10.1289/ehp.6000.

Li, X., Kuang, X.M., Yan, C., Ma, S., Paulson, S.E., Zhu, T., Zhang, Y., Zheng, M., 2019. Oxidative potential by PM2.5 in the North China Plain: generation of hydroxyl radical. Environ. Sci. Technol. 53 (1), 512–520. https://doi.org/10.1021/acs.est.8b05253.

Lin, P., Yu, J.Z., 2011. Generation of reactive oxygen species mediated by humic-like substances in atmospheric aerosols. Environ. Sci. Technol. 45 (24), 10362–10368. https://doi.org/10.1021/es2028229.

Lin, M., Yu, J.Z., 2019. Effect of metal-organic interactions on the oxidative potential of mixtures of atmospheric humic-like substances and copper/manganese as investigated by the dithiothreitol assay. Sci. Total Environ. 697, 134012. https://doi.org/10.1016/j.scitotenv.2019.134012.

Lin, M., Yu, J.Z., 2020. Assessment of interactions between transition metals and atmospheric organics: ascorbic acid depletion and hydroxyl radical formation in organic-metal mixtures. Environ. Sci. Technol. 54 (3), 1431–1442. https://doi.org/10.1021/acs.est.9b07478.

Lin, H., Chen, Q., Wang, M., Chang, T., 2022. Oxidation potential and coupling effects of the fractionated components in airborne fine particulate matter. Environ. Res. 213, 113652. https://doi.org/10.1016/j.envres.2022.113652.

Linxiang, L., Abe, Y., Nagasawa, Y., Kudo, R., Usui, N., Imai, K., Mashino, T., Mochizuki, M., Miyata, N., 2004. An HPLC assay of hydroxyl radicals by the hydroxylation reaction of terephthalic acid. Biomed. Chromatogr. 18 (7), 470–474. https://doi.org/10.1002/bmc.339.

Liu, Z., Lu, X., Feng, J., Fan, Q., Zhang, Y., Yang, X., 2017. Influence of ship emissions on urban air quality: a comprehensive study using highly time-resolved online measurements and numerical simulation in Shanghai. Environ. Sci. Technol. 51 (1), 202–211. https://doi.org/10.1021/acs.est.6b03834.

Liu, L., Urch, B., Szyszkowicz, M., Evans, G., Speck, M., Van Huang, A., Leingartner, K., Shutt, R.H., Pelletier, G., Gold, D.R., et al., 2018. Metals and oxidative potential in urban particulate matter influence systemic inflammatory and neural biomarkers: a controlled exposure study. Environ. Int. 121 (Pt 2), 1331–1340. https://doi.org/10.1016/j.envint.2018.10.055.

Lovett, C., Sowlat, M.H., Saliba, N.A., Shihadeh, A.L., Sioutas, C., 1994. Oxidative potential of ambient particulate matter in Beirut during Saharan and Arabian dust events. Atmos. Environ. 2018 (188), 34–42. https://doi.org/10.1016/j.atmosenv.2018.06.016.

Lyu, Y., Guo, H., Cheng, T., Li, X., 2018. Particle size distributions of oxidative potential of lung-deposited particles: assessing contributions from quinones and water-soluble metals. Environ. Sci. Technol. 52 (11), 6592–6600. https://doi.org/10.1021/acs.est.7b06686.

Ma, Y., Cheng, Y., Qiu, X., Cao, G., Kuang, B., Yu, J.Z., Hu, D., 2019. Optical properties, source apportionment and redox activity of humic-like substances (HULIS) in airborne fine particulates in Hong Kong. Environ. Pollut. 255 (Pt 1), 113087. https://doi.org/10.1016/j.envpol.2019.113087.

Maikawa, C.L., Weichenthal, S., Wheeler, A.J., Dobbin, N.A., Smargiassi, A., Evans, G., Liu, L., Goldberg, M.S., Pollitt, K.J., 2016. Particulate oxidative burden as a predictor of exhaled nitric oxide in children with asthma. Environ. Health Perspect. 124 (10), 1616–1622. https://doi.org/10.1289/EHP175.

Mancilla, Y., Araizaga, A.E., Mendoza, A., 2012. A tunnel study to estimate emission factors from mobile sources in Monterrey,Mexico. J. Air Waste Manag. Assoc. 62 (12), 1431–1442. https://doi.org/10.1080/10962247.2012.717902.

Mancilla, Y., Herckes, P., Fraser, M.P., Mendoza, A., 2015. Secondary organic aerosol contributions to PM2. 5 in Monterrey, Mexico: temporal and seasonal variation. Atmos. Res. 153, 348–359.

Mancilla, Y., Herckes, P., Fraser, M.P., Mendoza, A., 2015. Secondary organic aerosol contributions to PM2.5 in Monterrey, Mexico: temporal and seasonal variation. Atmos. Res. 153, 348–359. https://doi.org/10.1016/j.atmosres.2014.09.009.

McWhinney, R.D., Badali, K., Liggio, J., Li, S.M., Abbatt, J.P., 2013. Filterable redox cycling activity: a comparison between diesel exhaust particles and secondary organic aerosol constituents. Environ. Sci. Technol. 47 (7), 3362–3369. https://doi.org/10.1021/es304676x.

Ming, L., Jin, L., Li, J., Fu, P., Yang, W., Liu, D., Zhang, G., Wang, Z., Li, X., 2017. PM2.5 in the Yangtze River Delta, China: chemical compositions, seasonal variations, and regional pollution events. Environ. Pollut. 223, 200–212. https://doi.org/10.1016/j.envpol.2017.01.013.

Na, K., Sawant, A.A., Song, C., Cocker, D.R., 2004. Primary and secondary carbonaceous species in the atmosphere of Western Riverside County,California. Atmos. Environ. 38 (9), 1345–1355. https://doi.org/10.1016/j.atmosenv.2003.11.023.

Olechnowicz, J., Tinkov, A., Skalny, A., Suliburska, J., 2018. Zinc status is associated with inflammation, oxidative stress, lipid, and glucose metabolism. J. Physiol. Sci. 68 (1), 19–31. https://doi.org/10.1007/s12576-017-0571-7.

Pachon, J.E., Weber, R.J., Zhang, X., Mulholland, J.A., Russell, A.G., 2013. Revising the use of potassium (K) in the source apportionment of PM2.5. Atmos. Pollut. Res. 4 (1), 14–21. https://doi.org/10.5094/apr.2013.002.

Pope III, C.A., Turner, M.C., Burnett, R.T., Jerrett, M., Gapstur, S.M., Diver, W.R., Krewski, D., Brook, R.D., 2015. Relationships between fine particulate air pollution, cardiometabolic disorders, and cardiovascular mortality. Circ. Res. 116 (1), 108–115.

Prahalad, A.K., Inmon, J., Dailey, L.A., Madden, M.C., Ghio, A.J., Gallagher, J.E., 2001. Air pollution particles mediated oxidative DNA base damage in a cell free system and in human airway epithelial cells in relation to particulate metal content and bioreactivity. Chem. Res. Toxicol. 14 (7), 879–887.

Puthussery, J.V., Singh, A., Rai, P., Bhattu, D., Kumar, V., Vats, P., Furger, M., Rastogi, N., Slowik, J.G., Ganguly, D., et al., 2020. Real-time measurements of PM2.5 oxidative potential using a dithiothreitol assay in Delhi, India. Environ. Sci. Technol. Lett. 7 (7), 504–510. https://doi.org/10.1021/acs.estlett.0c00342.

Querol, X., Zhuang, X., Alastuey, A., Viana, M., Lv, W., Wang, Y., Lopez, A., Zhu, Z., Wei, H., Xu, S., 2006. Speciation and sources of atmospheric aerosols in a highly industrialised emerging mega-city in central China. J. Environ. Monit. 8 (10), 1049–1059. https://doi.org/10.1039/b608768j.

Robinson, D.L., 2017. Composition and oxidative potential of PM2.5 pollution and health. J. Thorac. Dis. 9 (3), 444–447. https://doi.org/10.21037/jtd.2017.03.92.

Saffari, A., Daher, N., Shafer, M.M., Schauer, J.J., Sioutas, C., 2014. Global perspective on the oxidative potential of airborne particulate matter: a synthesis of research findings. Environ. Sci. Technol. 48 (13), 7576–7583. https://doi.org/10.1021/es500937x.

Samara, C., 2017. On the redox activity of urban aerosol particles: implications for size distribution and relationships with organic aerosol components. Atmosphere 8 (12). https://doi.org/10.3390/atmos8100205.

Saran, M., Summer, K.H., 1999. Assaying for hydroxyl radicals: hydroxylated terephthalate is a superior fluorescence marker than hydroxylated benzoate. Free Radic. Res. 31 (5), 429–436. https://doi.org/10.1080/10715769900300991.

Shang, J., Zhang, Y., Schauer, J.J., Chen, S., Yang, S., Han, T., Zhang, D., Zhang, J., An, J., 2022. Prediction of the oxidation potential of PM2. 5 exposures from pollutant composition and sources. Environ. Pollut. 293, 118492.

Son, Y., Mishin, V., Welsh, W., Lu, S.E., Laskin, J.D., Kipen, H., Meng, Q., 2015. A novel high-throughput approach to measure hydroxyl radicals induced by airborne particulate matter. Int. J. Environ. Res. Public Health 12 (11), 13678–13695. https://doi.org/10.3390/ijerph121113678.

Strak, M., Janssen, N.A., Godri, K.J., Gosens, I., Mudway, I.S., Cassee, F.R., Lebret, E., Kelly, F.J., Harrison, R.M., Brunekreef, B., et al., 2012. Respiratory health effects of airborne particulate matter: the role of particle size, composition, and oxidative potential-the RAPTES project. Environ. Health Perspect. 120 (8), 1183–1189. https://doi.org/10.1289/ehp.1104389.

Tong, H., Arangio, A.M., Lakey, P.S.J., Berkemeier, T., Liu, F., Kampf, C.J., Brune, W.H., Pöschl, U., Shiraiwa, M., 2016. Hydroxyl radicals from secondary organic aerosol decomposition in water. Atmos. Chem. Phys. 16 (3), 1761–1771. https://doi.org/10.5194/acp-16-1761-2016.

Tong, H., Lakey, P.S.J., Arangio, A.M., Socorro, J., Shen, F., Lucas, K., Brune, W.H., Poschl, U., Shiraiwa, M., 2018. Reactive oxygen species formed by secondary organic aerosols in water and surrogate lung fluid. Environ. Sci. Technol. 52 (20), 11642–11651. https://doi.org/10.1021/acs.est.8b03695.

Verma, V., Ning, Z., Cho, A.K., Schauer, J.J., Shafer, M.M., Sioutas, C., 2009. Redox activity of urban quasi-ultrafine particles from primary and secondary sources. Atmos. Environ. 43 (40), 6360–6368. https://doi.org/10.1016/j.atmosenv.2009.09.019.

Verma, V., Fang, T., Guo, H., King, L., Bates, J.T., Peltier, R.E., Edgerton, E., Russell, A.G., Weber, R.J., 2014. Reactive oxygen species associated with water-soluble PM2.5 in the southeastern United States: spatiotemporal trends and source apportionment. Atmos. Chem. Phys. 14 (23), 12915–12930. https://doi.org/10.5194/acp-14-12915-2014.

Verma, V., Wang, Y., El-Afifi, R., Fang, T., Rowland, J., Russell, A.G., Weber, R.J., 2015. Fractionating ambient humic-like substances (HULIS) for their reactive oxygen species activity – assessing the importance of quinones and atmospheric aging. Atmos. Environ. 120, 351–359. https://doi.org/10.1016/j.atmosenv.2015.09.010.

Verma, V., Fang, T., Xu, L., Peltier, R.E., Russell, A.G., Ng, N.L., Weber, R.J., 2015. Organic aerosols associated with the generation of reactive oxygen species (ROS) by water-soluble PM2.5. Environ. Sci. Technol. 49 (7), 4646–4656. https://doi.org/10.1021/es505577w.

Wang, Y., Wang, M., Li, S., Sun, H., Mu, Z., Zhang, L., Li, Y., Chen, Q., 2020. Study on the oxidation potential of the water-soluble components of ambient PM2.5 over Xi'an, China: pollution levels, source apportionment and transport pathways. Environ. Int. 136, 105515. https://doi.org/10.1016/j.envint.2020.105515.

Wei, J., Yu, H., Wang, Y., Verma, V., 2019. Complexation of iron and copper in ambient particulate matter and its effect on the oxidative potential measured in a surrogate lung fluid. Environ. Sci. Technol. 53 (3), 1661–1671. https://doi.org/10.1021/acs.est.8b05731.

Wei, J., Fang, T., Shiraiwa, M., 2022. Effects of acidity on reactive oxygen species formation from secondary organic aerosols. ACS Environ.Au https://doi.org/10.1021/acsenvironau.2c00018.

Weichenthal, S.A., Lavigne, E., Evans, G.J., Godri Pollitt, K.J., Burnett, R.T., 2016. Fine particulate matter and emergency room visits for respiratory illness. Effect modification by oxidative potential. Am. J. Respir. Crit. Care Med. 194 (5), 577–586. https://doi.org/10.1164/rccm.201512-2434OC.

Weichenthal, S., Crouse, D.L., Pinault, L., Godri-Pollitt, K., Lavigne, E., Evans, G., van Donkelaar, A., Martin, R.V., Burnett, R.T., 2016. Oxidative burden of fine particulate air pollution and risk of cause-specific mortality in the Canadian census health and environment cohort (CanCHEC). Environ. Res. 146, 92–99. https://doi.org/10.1016/j.envres.2015.12.013.

Weichenthal, S., Lavigne, E., Evans, G., Pollitt, K., Burnett, R.T., 2016. Ambient PM2.5 and risk of emergency room visits for myocardial infarction: impact of regional PM2.5 oxidative potential: a case-crossover study. Environ. Health 15, 46. https://doi.org/10.1186/s12940-016-0129-9.

Wu, D., Zheng, H., Li, Q., Jin, L., Lyu, R., Ding, X., Huo, Y., Zhao, B., Jiang, J., Chen, J., et al., 2022. Toxic potency-adjusted control of air pollution for solid fuel combustion. Nat. Energy 7 (2), 194–202. https://doi.org/10.1038/s41560-021-00951-1.

Xiong, Q., Yu, H., Wang, R., Wei, J., Verma, V., 2017. Rethinking dithiothreitol-based particulate matter oxidative potential: measuring dithiothreitol consumption versus reactive oxygen species generation. Environ. Sci. Technol. 51 (11), 6507–6514. https://doi.org/10.1021/acs.est.7b01272.

Xu, X., Lu, X., Li, X., Liu, Y., Wang, X., Chen, H., Chen, J., Yang, X., Fu, T.M., Zhao, Q., et al., 2020. ROS-generation potential of humic-like substances (HULIS) in ambient PM2.5 in urban Shanghai: association with HULIS concentration and light absorbance. Chemosphere 256, 127050. https://doi.org/10.1016/j.chemosphere.2020.127050.

Xu, J.W., Martin, R.V., Evans, G.J., Umbrio, D., Traub, A., Meng, J., van Donkelaar, A., You, H., Kulka, R., Burnett, R.T., et al., 2021. Predicting spatial variations in multiple measures of oxidative burden for outdoor fine particulate air pollution across Canada. Environ. Sci. Technol. 55 (14), 9750–9760. https://doi.org/10.1021/acs.est.1c01210.

Yang, F., Liu, C., Qian, H., 2021. Comparison of indoor and outdoor oxidative potential of PM2.5: pollution levels, temporal patterns, and key constituents. Environ. Int. 155, 106684. https://doi.org/10.1016/j.envint.2021.106684.

Yang, C., Hong, Z., Chen, J., Xu, L., Zhuang, M., Huang, Z., 2022. Characteristics of secondary organic aerosols tracers in PM2.5 in three central cities of the Yangtze river delta, China. Chemosphere 293, 133637. https://doi.org/10.1016/j.chemosphere.2022.133637.

Yu, H., Wei, J., Cheng, Y., Subedi, K., Verma, V., 2018. Synergistic and antagonistic interactions among the particulate matter components in generating reactive oxygen species based on the dithiothreitol assay. Environ. Sci. Technol. 52 (4), 2261–2270.

Yu, S., Liu, W., Xu, Y., Yi, K., Zhou, M., Tao, S., Liu, W., 2019. Characteristics and oxidative potential of atmospheric PM2.5 in Beijing: source apportionment and seasonal variation. Sci. Total Environ. 650 (Pt 1), 277–287. https://doi.org/10.1016/j.scitotenv.2018.09.021.

Yu, H., Puthussery, J.V., Verma, V., 2019. A semi-automated multi-endpoint reactive oxygen species activity analyzer (SAMERA) for measuring the oxidative potential of ambient PM2.5 aqueous extracts. Aerosol Sci. Technol. 54 (3), 304–320. https://doi.org/10.1080/02786826.2019.1693492.

Yu, H., Puthussery, J.V., Wang, Y., Verma, V., 2021. Spatiotemporal variability in the oxidative potential of ambient fine particulate matter in the midwestern United States. Atmos. Chem. Phys. 21 (21), 16363–16386. https://doi.org/10.5194/acp-21-16363-2021.

Yu, G., Zhang, Y., Yang, F., He, B., Zhang, C., Zou, Z., Yang, X., Li, N., Chen, J., 2021. Dynamic Ni/V ratio in the ship-emitted particles driven by multiphase fuel oil regulations in coastal China. Environ. Sci. Technol. 55 (22), 15031–15039. https://doi.org/10.1021/acs.est.1c02612.

Yuan, Q., Lai, S., Song, J., Ding, X., Zheng, L., Wang, X., Zhao, Y., Zheng, J., Yue, D., Zhong, L., et al., 2018. Seasonal cycles of secondary organic aerosol tracers in rural Guangzhou, Southern China: the importance of atmospheric oxidants. Environ. Pollut. 240, 884–893. https://doi.org/10.1016/j.envpol.2018.05.009.

Zhang, F., Zhao, J., Chen, J., Xu, Y., Xu, L., 2011. Pollution characteristics of organic and elemental carbon in PM2.5 in Xiamen, China. J. Environ. Sci. 23 (8), 1342–1349. https://doi.org/10.1016/s1001-0742(10)60559-1.

Zhang, X., Staimer, N., Tjoa, T., Gillen, D.L., Schauer, J.J., Shafer, M.M., Hasheminassab, S., Pakbin, P., Longhurst, J., Sioutas, C., et al., 2016. Associations between microvascular function and short-term exposure to traffic-related air pollution and particulate matter oxidative potential. Environ. Health 15 (1), 81. https://doi.org/10.1186/s12940-016-0157-5.

Zhang, X., Zhang, Y., Liu, Y., Zhao, J., Zhou, Y., Wang, X., Yang, X., Zou, Z., Zhang, C., Fu, Q., et al., 2019. Changes in the SO2 level and PM2.5 components in Shanghai driven by implementing the ship emission control policy. Environ. Sci. Technol. 53 (19), 11580–11587. https://doi.org/10.1021/acs.est.9b03315.

Zhu, C.-S., Chen, C.-C., Cao, J.-J., Tsai, C.-J., Chou, C.C.K., Liu, S.-C., Roam, G.-D., 2010. Characterization of carbon fractions for atmospheric fine particles and nanoparticles in a highway tunnel. Atmos. Environ. 44 (23), 2668–2673. https://doi.org/10.1016/j.atmosenv.2010.04.042.

Zong, Z., Wang, X., Tian, C., Chen, Y., Qu, L., Ji, L., Zhi, G., Li, J., Zhang, G., 2016. Source apportionment of PM 2.5 at a regional background site in North China using PMF linked with radiocarbon analysis: insight into the contribution of biomass burning. Atmos. Chem. Phys. 16 (17), 11249–11265.